Available online at www.sciencedirect.com

SCIENCE DIRECT®

ELSEVIER

Coordination Chemistry Reviews 249 (2005) 329–341

COORDINATION CHEMISTRY REVIEWS

www.elsevier.com/locate/ccr

Review

Related rhenium(V) catalysts adopt different mechanisms for oxygen atom transfer

James H. Espenson*

Ames Laboratory and Department of Chemistry, Iowa State University of Science and Technology, 25 Speeding Hall, Ames, Iowa 50011, USA

Received 2 February 2004; accepted 24 June 2004
Available online 15 September 2004

Contents

---

* Tel.: +1 515 294 5730; fax: +1 515 294 233.
E-mail address: espenson@iastate.edu.

0010-8545/$ – see front matter © 2004 Elsevier B.V. All rights reserved.
doi:10.1016/j.ccr.2004.06.018

Abstract

The chemical mechanisms for three related rhenium(V) catalysts of oxygen atom transfer reactions are reviewed. Two of the catalysts are compounds with a single rhenium atom, [MeReE(mtp)(PPh3)], where E is either O (**1**) or S (**2**) and mtpH_2 is 2-(mercaptomethyl)thiophenol; the third is the di-rhenium compound $\{MeReO(mtp)\}_2$ (**3**). In each of them, the Re atom is square-pyramidal, sitting slightly above the approximate basal plane defined by S, S, C, and P; the oxo or thio group occupies the axial position. They all catalyze oxygen atom transfer from pyridine *N*-oxides to PAr_3. The reaction rates are in the orders **3** ≫ **1** ≫ **2**; even more striking is that the rate laws for the trio of catalysts is distinctly different. This signals the intervention of different chemical steps and intermediates.

© 2004 Elsevier B.V. All rights reserved.

Keywords: Heterocycles; Ligand; Catalyst; Oxygen atom transfer

1. Introduction

Henry Taube has contributed to the field of inorganic reaction mechanisms in so many ways that it is difficult to describe his contributions succintly. I shall not try to do so, because I am presenting work on a theme that builds on Taube's research from an early stage of his career, where the focus was on oxygen chemistry. I am of an age that I can allow myself to reminisce briefly. My first personal encounter with Taube was in 1959; I had just completed my second year in graduate school at the University of Wisconsin, with Edward L. King as my mentor, when Taube came from the University of Chicago to Madison to present a week-long series of summer lectures. This was just when his seminal research on inner-sphere electron transfer was first appearing. I remember a comment Taube made at the start of his first lecture, to the effect that much of his career had been devoted to oxygen chemistry in one way or another. Those who recall his early studies of ozone reactivity [1], oxygen-exchange and other reactions of oxoanions [2], redox reactivity of species such as oxalic and formic acids [3], and water exchange [4] can see the truth of that perception. Indeed, by an excellent turn of fate, I was later privileged to engage in postdoctoral research with Taube shortly after his move to Stanford University. As fate would further have it, my year there was spent on, what else?, oxygen chemistry; particularly a series of oxygen-18 tracer experiments on the ozone oxidation of species such as sulfite and nitrite ions, manganese(II) and thallium(I) [5].

One further historical reference appears in order. I recall appreciating at the time of its publication the title of a perceptive article by W.P. Jencks intriguingly entitled "*How Does a Reaction Choose Its Mechanism?*" [6] That thought is pertinent to this presentation which deals for the most part with a single reaction that adopts different mechanisms when it is catalyzed by one or another of seemingly similar rhenium(V) compounds. Indeed, the composition and structural similarities among these catalysts are so great as to make the divergent mechanisms all the more astonishing.

2. The test reaction

The deoxygenation of nitrogen heterocycles, particularly pyridine *N*-oxides, with phosphines was chosen as the standard for assessing catalytic mechanisms in this work. This reaction holds some inherent interest for the synthesis of heterocycles [7], for which other procedures are sometimes disadvantageous [8]. Its catalysis by rhenium compounds offers attractive features: the rhenium compounds are easily prepared, stable for long periods, and unreactive towards oxygen and traces of moisture. Thus benchtop protocols are used.

In a general sense these formulas will be used for reactants and products, PyO, PZ_3, Py, and Z_3PO; formulas for specific compounds will be used where appropriate. The net reaction is spontaneous; to cite thermodynamic data for particular reaction partners, we have [9]

$$\begin{aligned}&4\text{-MeC}_5\text{H}_4\text{NO} + \text{PPh}_3 \rightarrow 4\text{-MeC}_5\text{H}_4\text{N} + \text{Ph}_3\text{PO},\\&\Delta H^\circ(\cong \Delta G^\circ) = -266\,\text{kJ}\end{aligned} \tag{1}$$

Perhaps the best reason for selecting this reaction is that it does not occur to any extent without a catalyst, insofar as we have been able to determine in experiments lasting more than two months. Arguably, the reaction does not occur in practice because the reactants are closed-shell (octet rule) species. Further, as a reviewer suggested, PyO itself has a polarization such that the oxygen is too electron rich to be attacked nucleophically; on the other hand, as shown by the mechanistic data presented herein, activation by high-valent rhenium compounds greatly reduces the electron density on the oxygen atom. Indeed, with a suitable rhenium catalyst the reaction occurs readily, proceeding to completion with the precise stoichiometry indicated. The catalyst survives intact, usually well beyond the end of the reaction. In certain cases, however, the catalyst may itself react with either PyO or PZ_3, and thus be converted to a different form, which usually is noncatalytic. Such a reaction may sometimes affect the design of the experiment, indicating for example, a preferable order of mixing of reagents.

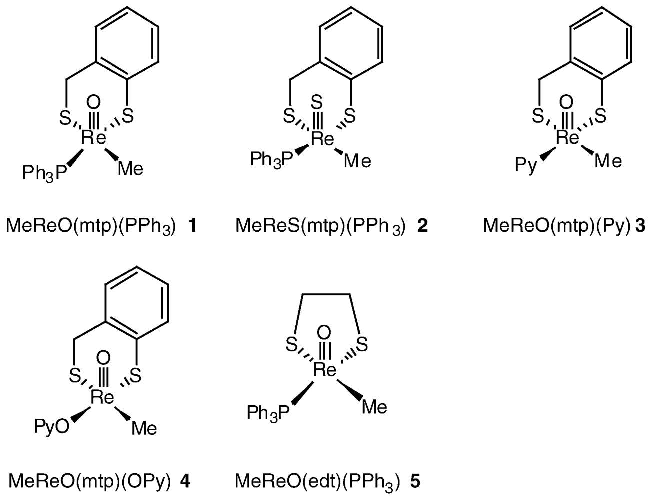

MeReO(mtp)(PPh$_3$) **1** MeReS(mtp)(PPh$_3$) **2** MeReO(mtp)(Py) **3**

MeReO(mtp)(OPy) **4** MeReO(edt)(PPh$_3$) **5**

Plate 1. Structural formulas of five-coordinate catalysts and their derivatives.

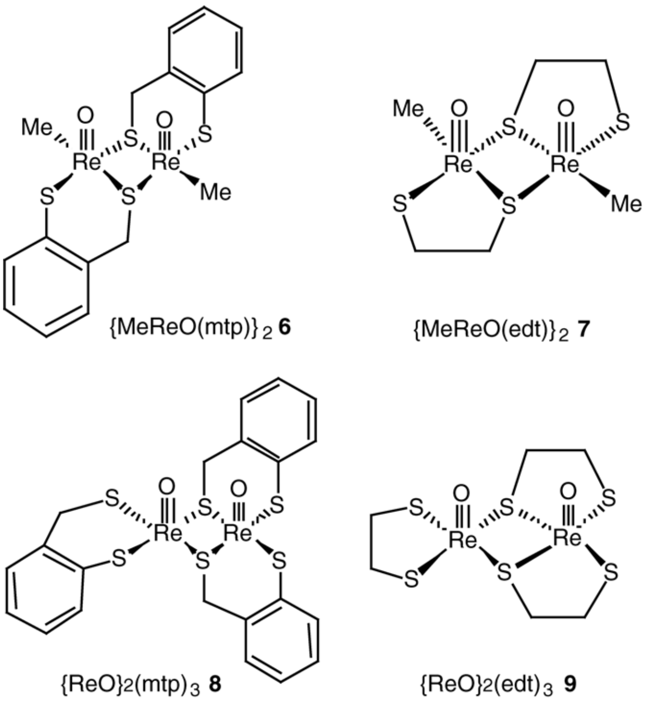

{MeReO(mtp)}$_2$ **6** {MeReO(edt)}$_2$ **7**

{ReO}$_2$(mtp)$_3$ **8** {ReO}$_2$(edt)$_3$ **9**

Plate 2. Structural formulas of dirhenium catalysts.

3. The catalysts

The catalysts divide into several groups, as follows. Compounds **1**–**5** have the general formula MeReE(dithiolate)(L), where E is O (usually) or S, the dithiolate is 2-mercaptomethyl(thiophenolate), mtp, 1,2-ethanedithiolate, edt, or 1,3-propanedithiolate, pdt, and L is a ligand such as pyridine or phosphine. The structural formulas of some of these compounds are shown in Plate 1. There are two types of dirhenium catalysts, {MeReO(dithiolate)}$_2$, **6**–**7**, and {ReO}$_2$(dithiolate)$_3$, **8**–**9**, as depicted in Plate 2. The final group comprises otherwise similar six-coordinate compounds, **10**–**14**, of which only **10** and **11** catalyze reaction (1).

These compounds have been synthesized in pure form and fully characterized, including by X-ray crystallography. The

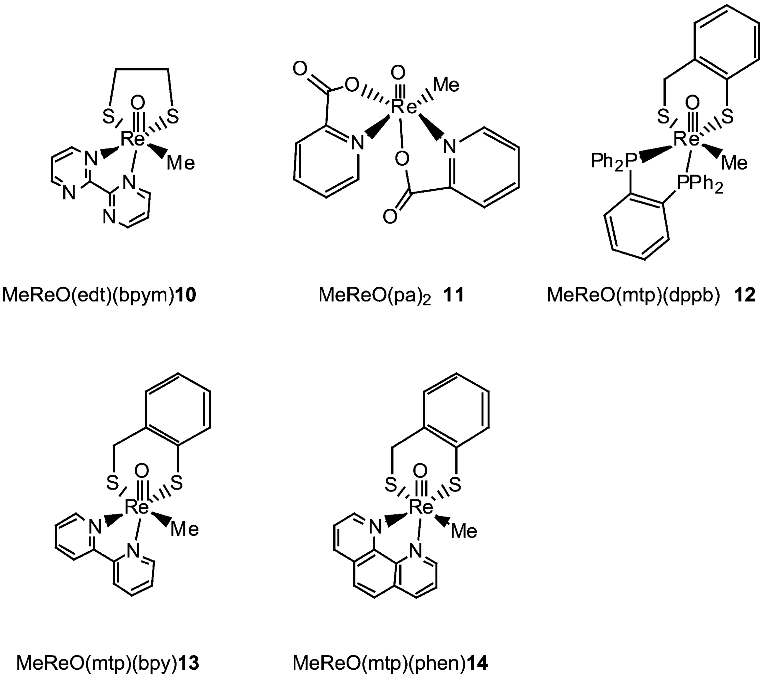

MeReO(edt)(bpym)**10** MeReO(pa)$_2$ **11** MeReO(mtp)(dppb) **12**

MeReO(mtp)(bpy)**13** MeReO(mtp)(phen)**14**

Plate 3. Six coordinate oxorhenium(V) compounds.

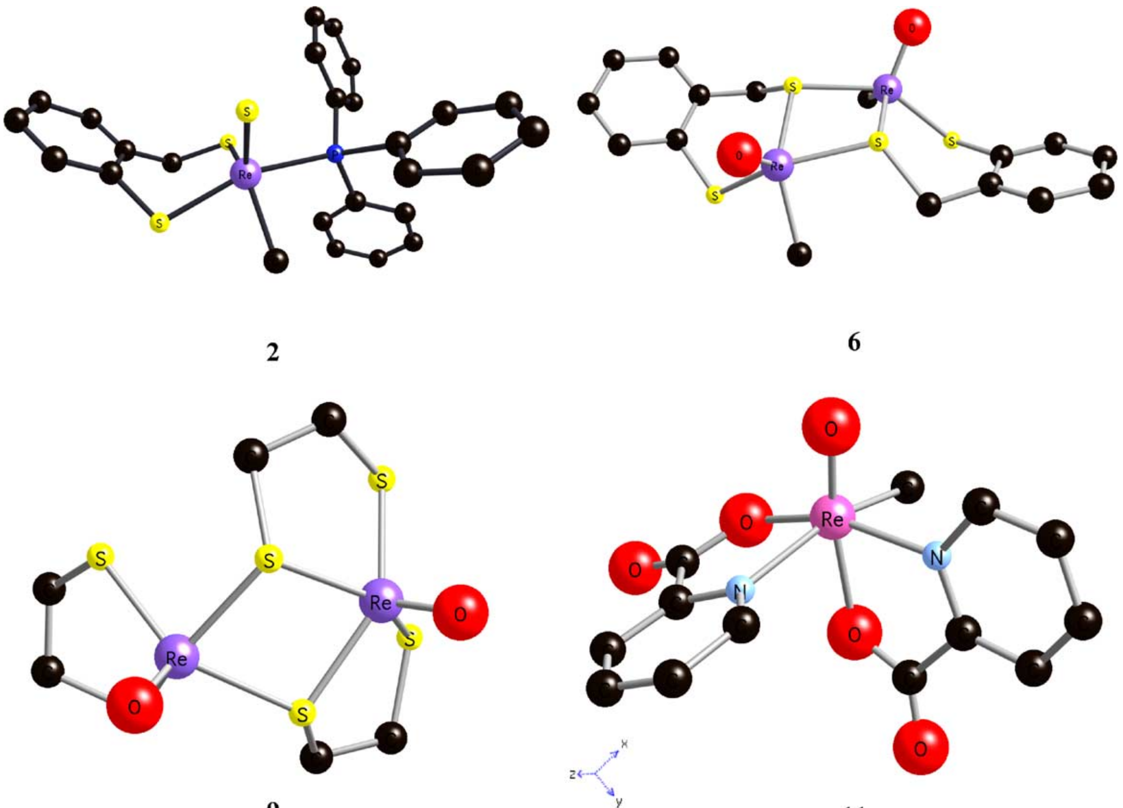

2 **6** **9** **11**

Plate 4. Representation of the crystal and molecular structures of oxo-rhenium(V) catalysts **2**, **6**, **9**, and **11**, as drawn by the program CrystalMaker [10].

molecular structures of a representative sample of catalysts: **2**, **6**, **9**, and **11** are presented in Plate 4.

4. Catalysts 1 and 2

The compounds first to be considered as catalysts are MeReO(mtp)PPh$_3$, **1**, and MeReS(mtp)PPh$_3$, **2**. Both carry reaction (1) to completion, but **1** is much more active. On the other hand, **1** is by no means the most active catalyst for reaction (1), as will be demonstrated later. To illustrate the relative effectiveness of **1** versus **2**, consult Fig. 1A and B, which present concentrations of PyO as a function of time, as determined by UV spectroscopy.

Quantitative kinetic data were obtained by the UV method for the most part, on the basis of $\varepsilon_{\text{PicO}}$ = 945 L mol^{-1} cm^{-1} at 330 nm. The rate laws for the two are not only remarkably different, but each form indicates considerable mechanistic complexity.

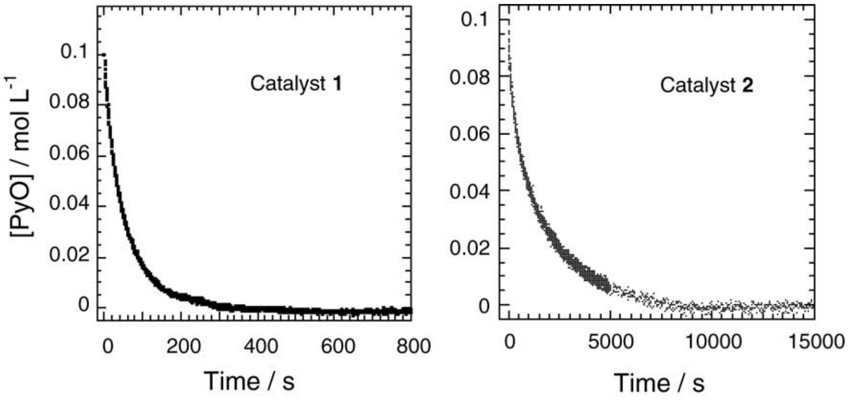

Fig. 1. Progress curves for the reaction between 4-MeC$_5$H$_4$NO and PPh$_3$ at 25 °C in benzene as catalyzed by **1** and by **2**. Concentrations were: 0.10 mmol L^{-1} of 4-MeC$_5$H$_4$NO, 5.2 mmol L^{-1} of PPh$_3$, and 0.078 mmol L^{-1} of **1** or **2**.

$$-\frac{\mathrm{d}[\mathrm{PyO}]}{\mathrm{d}t} = k_1\frac{[\mathbf{1}][\mathrm{PyO}]^2}{[\mathrm{PPh_3}]} \tag{2}$$

$$-\frac{\mathrm{d}[\mathrm{PyO}]}{\mathrm{d}t} = k_{2\mathrm{a}}[\mathbf{2}][\mathrm{PyO}]^{1/2} \tag{3}$$

The rate constants in benzene at 25 °C are $k_1 = 1.5 \times 10^4\,\mathrm{L\,mol^{-1}\,s^{-1}}$ for 4-MeC_5H_4NO and $1.8\,\mathrm{L\,mol^{-1}\,s^{-1}}$ for 4-NO_2-2-MeC_5H_4NO with **1** [11] and $k_{2a} = 0.68 \pm 0.02\,\mathrm{L^{1/2}\,mol^{-1/2}\,s^{-1}}$ and $(3.5 \pm 0.1) \times 10^{-3}\,\mathrm{L^{1/2}\,mol^{-1/2}\,s^{-1}}$ for **2** [12] with the same reagent pair. Actually, catalyst **2** follows Eq. (3) only at relatively high $[PPh_3] \geq 1\,\mathrm{mmol\,L^{-1}}$; below that the rate equation (and the mechanism) changes to the same form as in followed by **1**, in Eq. (2).

4.1. Catalysis by 1

4.1.1. Reaction scheme

The reactions with **1** (see Scheme 1) are inferred from the rate law, noting that PPh_3 is the product of a prior equilibrium, that one PyO is deoxygenated but a second is needed to complete the reaction, and that a dioxorhenium(VII) intermediate is formed in the rate-controlling step. According to this scheme, $k_1 = K_1k_2$. Validation of each aspect of the proposed chemical mechanism was sought, and in every case obtained.

First, ligand displacement reactions as in the K_1 step are known for many ligands that do not undergo further reactions; such ligands include pyridines, dialkyl sulfides, and other phosphines [13,14]. The ligand substitution reactions are of interest in their own right because the data signify a complex mechanism that proceeds by turnstile rotation [15]. Nonetheless, this review will not deal with the mechanistic aspects of the K_1 step because it remains at equilibrium during the catalysis of reaction (1), and its mechanism is therefore not pertinent. The point is simply to note that this step, inferred from the rate equation, represents precedented chemistry.

4.1.2. Nucleophilic assistance

This naturally raises the question of why two PyO's are needed to reach the transition state. It appears that the additional PyO assists N–O bond-breaking by acting as a nucleophile:

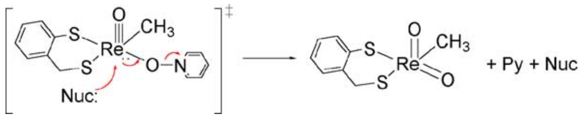

In support of that model, when bromide ions or pyridine is added, the rate is additionally accelerated. Further, the rate law with a family of ring-substituted pyridines then takes on a new form,

$$-\frac{\mathrm{d}[\mathrm{PyO}]}{\mathrm{d}t} = k_{\mathrm{N}}\frac{[\mathbf{1}][\mathrm{PyO}][\mathrm{RC_5H_4N}]}{[\mathrm{PPh_3}]} \tag{4}$$

The values of k_N correlate with the Hammett σ-constants. The reaction constants are $\rho = -2.7$ for 4-MeC_5H_4NO and -1.0 for 4-NO_2-2-MeC_5H_4NO. The negative values of ρ support the assignment of the accelerating affects of the pyridines to their role as nucleophiles in the mechanism.

4.1.3. Dioxorhenium(VII)

Third, considerable evidence has accumulated for the formation of a transient dioxorhenium(VII) intermediate. For one thing, it can be prepared from **1** and several O-donor compounds (4-MeC_5H_4NO, dmso, *tert*-butyl hydroperoxide, and PyO), when the product is stabilized by an excess of 4-picoline. Thus at −40 °C the compound $MeRe^{VII}(O)_2$(mtp)(4-Pic) was characterized by ^{1}H NMR; the spectrum is the same irrespective of which O-donating reagent was used, which shows that neither a fragment of that reagent nor any PPh_3 remains as a constituent of the transient. For another, the reactivity of $MeRe^{VII}(O)_2$(mtp) could be assessed quantitatively by competition experiments that utilized simultaneously a pair of phosphines, say PPh_3 and $PTol_3$. The concurrent formation of Ph_3PO and Tol_3PO provides the rate constants k_4 for a fast step in Scheme 1, relative to a standard which we took to be PPh_3. Further, it has proved possible to prepare two analogs of $MeRe^{VII}(O)_2$(mtp), with alkoxide-thiolate centers in place of the dithiolate; they are $MeRe(O)_2[\kappa^2\text{-}OCH_2C(H)RS\text{–}]$, R = H or Me [16]. These compounds can be isolated at room temperature, and their phosphine reactions were studied by direct kinetics.

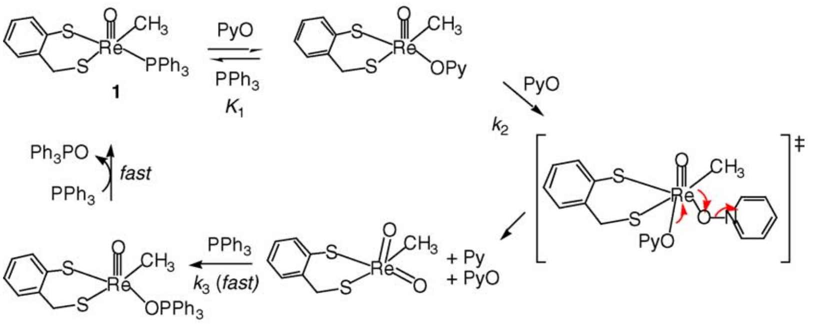

Scheme 1. Proposed mechanism for catalysis by **1**.

Scheme 1 concludes with a final ligand substitution step in which PPh_3 displaces Ph_3PO, restoring catalyst **1**. Further discussion of that rapid step in unnecessary. When the rhenium species are followed by NMR during the catalysis, only **1** was detected. All the other forms remain at low (steady-state) concentrations.

4.1.4. Substituent effects with ***1***

Different experiments were used to assess the extent and direction of electron flow in different reaction steps. In each case, the data correlate with the Hammett σ-constant. When the catalytic kinetics were studied with different $P(C_6H_4\text{-}4\text{-}R)_3$ reagents, the reaction constant derived from the variation of k_1 is $\rho_1 = +1.03$, consistent with PAr_3 being a leaving group in the first step. When $4\text{-}RC_5H_4NO$ substrates were used, the reaction constant proved to be unusually large, $\rho_1 = -3.8$. The value of k_c, which in this model is K_1k_2, reflects the role of PyO in steps 1 and 2. In each of those steps, PyO has been postulated to act nucleophilically; consistent with that, the reaction constant (which is $\rho_c = \rho_{K1} + \rho_{k3}$) is a large, negative number. A further implication is that the pyridine–oxygen bond scission makes but a small offsetting contribution to ρ_{k2}, because ρ_1 would other wise be less negative than was found. This implies that Py–O bond cleavage is not well advanced; the reaction proceeds via an early transition state.

Finally, the competition kinetics FOR k_4 (rel.) was evaluated for different $P(C_6H_4\text{-}4\text{-}R)_3$. Here, $\rho_3 = -0.7$; again, this is consistent with the phosphine attacking nucleophilically at the oxo group of the dioxorhenium(VII) intermediate.

4.2. Catalysis by ***2***

4.2.1. Half-order kinetics

With catalyst **2**, the half-order dependence on [PyO] can be accommodated only by a chain mechanism. It is always possible, however, that a line segment taken over a limited range of [PyO] might approximate half-order to the extent that an erroneous reaction order might be assigned. For example, if the kinetic dependence has the form $v = a[PyO]/\{b + [PyO]\}$, there will be a limited range of [PyO] over which the rate may appear to depend on $[PyO]^{1/2}$, particularly when one considers any imprecision in the rate measurements. To verify the authenticity of the $[PyO]^{1/2}$ dependence, the reaction rates were evaluated over a large range of [PyO], more than a 10^4-fold variation. Fig. 2 illustrates the half-order dependence over the entire range. In addition to initial rate studies, many experiments were followed over the full time course, giving results that fit closely to the integrated rate law for half-order kinetics.

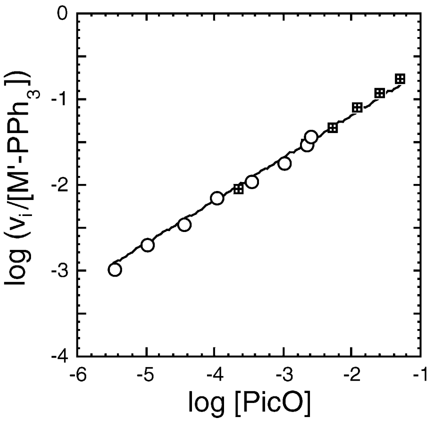

Fig. 2. Dependence of the initial rate on the initial concentration of $4\text{-}MeC_5H_4NO$ shown in the form of a log–log plot for data (NMR, hatched squares; UV, circles) obtained in benzene at 25.0 °C. In these experiments, [**2**] was (2.3–3.7) × 10^{-5} mol L^{-1} and $[PPh_3] \geq 3.5 \times 10^{-3}$ mol L^{-1}. The least-squares slope of the line is 0.53.

4.2.2. Chemical mechanism for ***2***

Scheme 2 presents a group of five chemical reactions that are in accord with the kinetics, and it presents postulated structures of the reaction intermediates. The three propagation steps involve the repeated cycling of three intermediates ($\mathbf{I}_1$, $\mathbf{I}_2$, and $\mathbf{I}_3$) in reactions that are more rapid than termination. From this scheme one can use the steady-state and long-chain approximations to derive this rate law:

$$-\frac{d[PyO]}{dt} = k_1^{prop}[I_1]_{ss}[PPh_3] = \sqrt{\frac{K_1 k_{init} k_1^{prop} k_2^{prop}}{k_{term}}}[\mathbf{2}][PyO]^{1/2} \qquad (5)$$

For the scheme to be credible, the intermediates and their reactions must be plausible, as judged on their (proposed) structures and on the known chemistry of rhenium compounds of this general character. Here we explore this matter. Step [3] represents the plausible addition of a ligand to the four-coordinate species $\mathbf{I}_1$ to produce five-coordinate $\mathbf{I}_3$, which is the geometrical isomer of **2**. Geometrical isomers of this type have been authenticated, and they do indeed lie on the pathway of ligand substitution reactions because

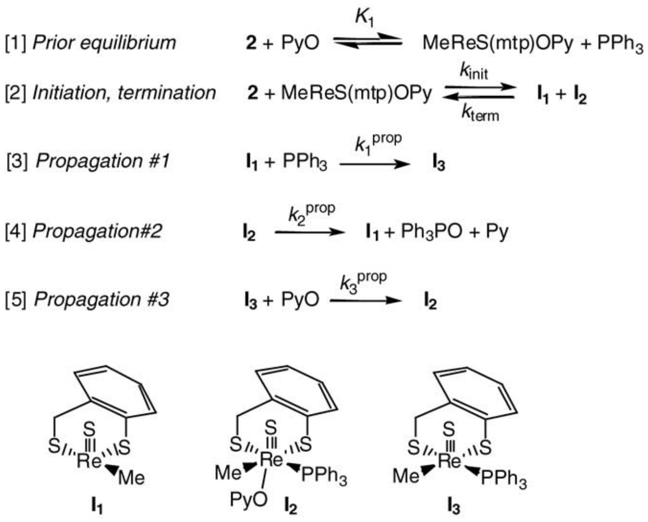

Scheme 2. Chain mechanism for catalysis by **2**.

of requirements arising from the principle of microscopic reversibility [15]. Step [5] depicts the formation of a six-coordinate rhenium(V) compound, a step common to **1** as well, as in Scheme 1; the PyO added here will provide nucleophilic assistance. Step [4] shows the assistance of the PyO nucleophile added in Step [5] on cleavage of the N–O bond, which releases Py and the nucleophile; Step [4] also has its counterpart Scheme 1. The propagation steps are outlined in structural terms in Scheme 3.

As noted, Schemes 1 and 2 have steps in common: the prior equilibrium and the nucleophile-assisted cleavage of the Py–O. Where the mechanisms differ is more interesting. First, there is no known oxo analogue of the four-coordinate species $\mathbf{I}_1$ in the oxo system, not even as a transient in this or other reactions. Second, the initiation–termination step has no precedent in the catalytic scheme for **1**, in addition to which it seems a rather peculiar transformation, in which two five-coordinate species, which are usually the most stable forms, are being converted to a six- and a four-coordinate species.

In fact, it is not far-fetched at all, because it finds a nearly exact parallel in the well-studied mechanism for the dimerization/monomerization reaction:

$$\begin{aligned}&\mathrm{MeReO(mtp)L}^{i} + \mathrm{MeReO(mtp)L}^{j}\\&\quad = \{\mathrm{MeReO(mtp)}\}_2(\mathbf{6}) + \mathrm{L}^{i} + \mathrm{L}^{j}\end{aligned} \tag{6}$$

This aspect of the chemistry is illustrated in Scheme 3, from which one can see that no new transformation need be introduced to account for Step [2] in the chain mechanism proposed for catalysis by **2**.

4.2.3. *A second pathway for 2*

It was remarked earlier that the chain mechanism no longer prevails for **2** at lower concentrations of $\mathrm{PPh_3}$ (roughly 10^{-3} mol L^{-1}, but dependent on [PyO]). The full rate law for catalyst **2**, both pathways included, is

$$-\frac{\mathrm{d[PyO]}}{\mathrm{d}t} = k_{2a}[\mathbf{2}][\mathrm{PyO}]^{1/2} + k_{2b}\frac{[\mathbf{2}][\mathrm{PyO}]^2}{[\mathrm{PPh_3}]} \tag{7}$$

with k_{2b} = 4.30 (4-$\mathrm{MeC_5H_4NO}$) and 3.3×10^{-3} (4-$\mathrm{NO_2C_5H_4NO}$) L mol^{-1} s^{-1} in benzene at 25 °C. The values of k_1 given earlier are some three orders of magnitude larger along the same pathway. Examination of Scheme 1 suggests why that may be so. The equilibrium constant K_1, representing coordination of PyO to rhenium, is likely to be larger for ReO than for ReS because of the electronegativity difference. Given that k_1 and k_{2b} are expressed as K_1k_2 the reactivity $\mathbf{1} \gg \mathbf{2}$ can thus be accounted for.

5. Catalyst 6

The dimer {MeReO(mtp)}$_2$ (**6**) is a much more reactive catalyst than its monomeric counterparts, such as MeReO(mtp)$\mathrm{PPh_3}$, **1**. It is useful to note that these species are related to one another by this reaction:

$$\{\mathrm{MeReO(mtp)}\}_2(\mathbf{6}) + 2\mathrm{PPh_3} = 2\mathrm{MeReO(mtp)PPh_3}(\mathbf{1}) \tag{8}$$

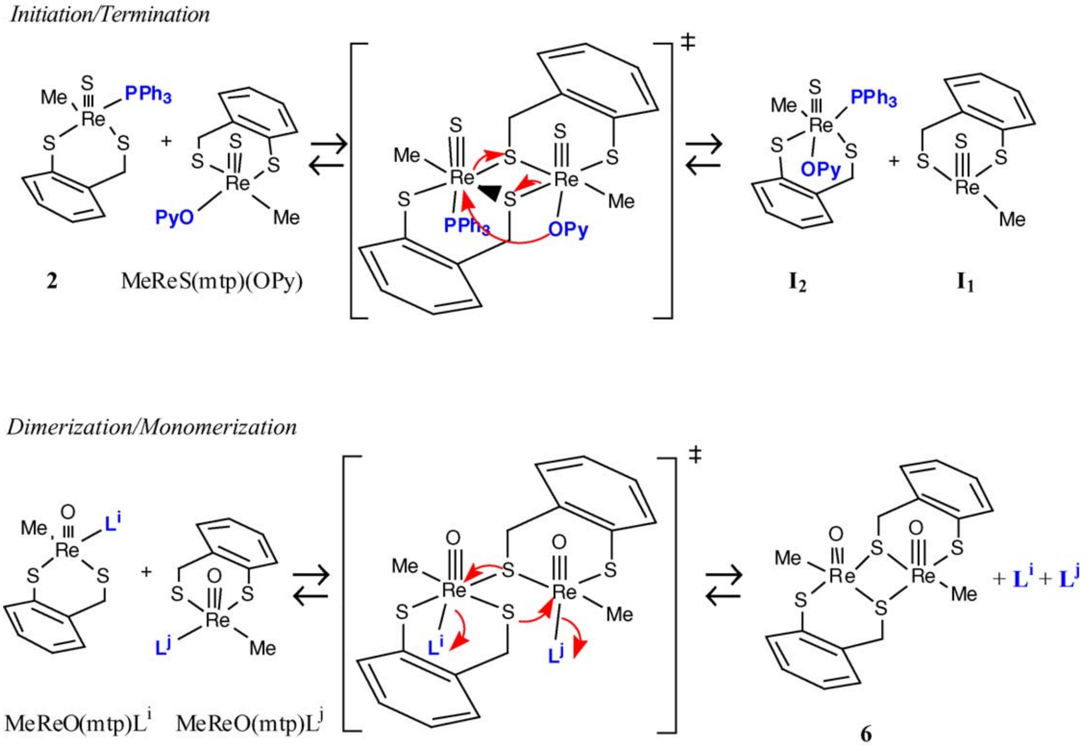

Scheme 3. Initiation/termination as compared with dimerization/monomerization.

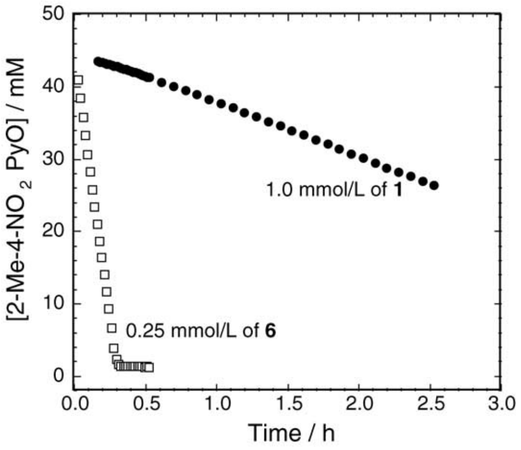

Fig. 3. The disappearance of 44.4 mmol L^{-1} of 2-methyl-4-nitropyridine N-oxide in solutions with 44.4 mmol L^{-1} of PPh$_3$, with catalysts **1** and **6**.

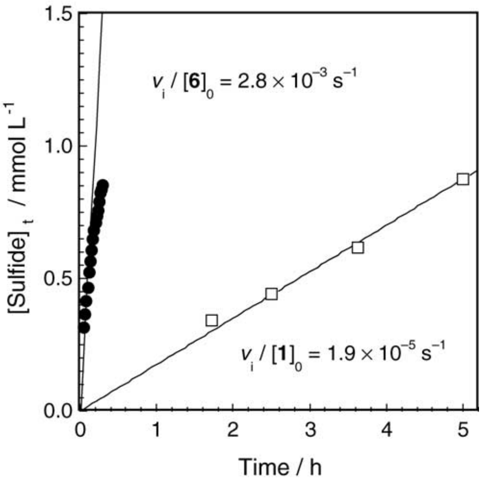

Fig. 4. Comparison of rhenium catalysts **6** and **1** for reaction (8) in C_6D_6 at 23 °C. Initial concentrations: 0.5 mmol L^{-1} of **6**, 19 mmol L^{-1} of MeS(O)Ph, and 22 mmol L^{-1} of PPh$_3$; 2.6 mmol L^{-1} of **1**, 26 mmol L^{-1} of MeS(O)Ph, and 28 mmol L^{-1} of PPh$_3$.

This reaction is an equilibrium, but it established slowly in the systems now under consideration, and thus **6** retains its identity. Indeed, one cause for the reactivity pattern **6** ≫ **1** lies in the avoidance of the step in which tightly-bound PPh$_3$ is removed from **1**; see the first step in Scheme 1.

5.1. *Reaction of 2-Me-4-NO$_2$C$_5$H$_4$NO*

Fig. 3 shows progress curves for the reaction of 2-Me-4-NO$_2$C$_5$H$_4$NO with PPh$_3$, comparing catalysts **6** and **1** [11]. The rate difference amounts to a factor of about 90 per mole of catalyst in favor of **6**.

5.2. *Me$_2$SO substrate*

5.2.1. *Catalytic rates, **6** versus **1***

Closely related to reaction (1) is the deoxygenation of sulfoxides such as methyl phenyl sulfoxide with a phosphine, which has been thoroughly studied [17], reaction (8):

$$\text{MeS(O)Ph} + \text{PPh}_3 \rightarrow \text{MeSPh} + \text{Ph}_3\text{PO} \tag{9}$$

As with reaction (1), **6** proved to be much more effective than **1** in terms of the initial rate of reaction (8). Fig. 4 shows the buildup of MeSPh with each catalyst, and establishes that the reactivity ratio of the two as ca. 150 per mol of catalyst in favor of **6**.

5.2.2. *Conversion of **6** to **1***

Careful examination of Fig. 4 shows that the reaction with **6** begins to die off at an early stage. This has been traced to the conversion of **6** to **1**, as in reaction (7). The loss of the most active catalyst is further exaggerated because the rate of monomerization of **6** is ca. 10-times faster when MeS(O)Ph is present; the rate law then includes a third, sulfoxide-dependent term:

$$-\frac{d[\mathbf{6}]}{dt} = \left\{ k_a[\text{PPh}_3] + k_b[\text{PPh}_3]^2 + \frac{kK_{6S}[\text{MeS(O)Ph}][\text{PPh}_3]}{1 + K_{6S}[\text{MeS(O)Ph}]} \right\} [\mathbf{6}] \tag{10}$$

The transition state for the extraordinary third term is worth depicting, because it relates to that for oxygen atom transfer, as will be described shortly.

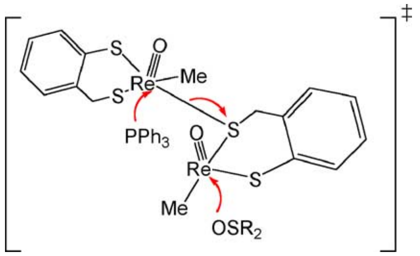

One might ask whether this scheme can also accomplish oxygen atom transfer, but the answer is negative. Two transition states resembling this one, but not identical with it, carry out the oxygen atom transfer reaction.

5.2.3. *Kinetics of reaction (8)*

The transition states for reaction (8) do, however, bear some similarity to the one shown above for monomerization of **6**. The rate law requires allowance for the nearly irreversible conversion of **6** to **1**, which is essentially nonreactive on this time scale. The rate law for the formation of RSR′ is [17]

$$\frac{d[\text{RSR}']}{dt} = \left\{ \frac{k_0 + k_1 K[\text{PAr}_3]}{1 + K[\text{PAr}_3]} \right\} K_{6P}[\text{MeS(O)Ph}][\mathbf{6}]_{T,t} \tag{11}$$

5.2.4. *Internal and external pathways*

This rate equation reveals two concurrent and competitive pathways for reaction (8). The parallel transition states that are inferred from Eq. (11) can be depicted as:

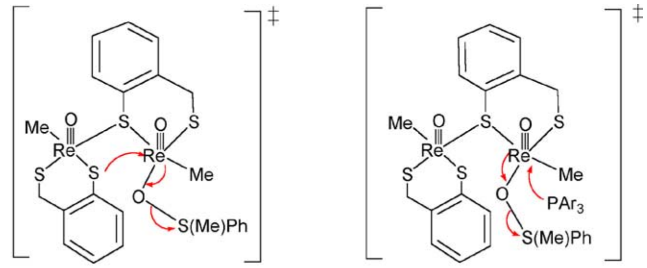

Internally-Assisted Transition State Externally-Assisted Transition State

One again notes that a coordination number below five is not involved. In both cases, the next form is a reactive dioxorhenium(VII) species, still a part of a di-rhenium species. Attack by PPh_3 abstracts an oxo group, allowing **6** to reassemble. If the one remaining μ–S bond is broken, however, the compound reverts to **1** with PPh_3 present, and catalytic activity falls substantially.

Catalysis by **6** offers a considerable advantage over that by **1**; the displacement of the bulky and tightly-coordinated phosphine by sulfoxide is not involved. With that major barrier absent, one can understand why **6** is so active compared to **1**.

The chemical mechanisms deserve further comment. As to monomerization, an added pathway is provided when sulfoxide is present. Sulfoxides alone, however, do not monomerize **6**; instead, they give the adduct **6**–OSR_2, the structure of which has been determined by X-ray analysis [13]. Although PPh_3 coordinates to **6**, the equilibrium constant is so small that the adduct cannot be readily detected. With both R_2SO and PPh_3 present, however, the mixed adduct, **6**($-OSR_2, -PPh_3$) can be detected directly by NMR. This signifies an important interaction, which is expressed in terms of a ternary complex in which one (only) of the S → Re bonds of the central core has been broken. We speculate that the two halves of the dimer can rotate about the remaining S–Re bonds joining the two subunits, so as to allow room for the sterically-encumbered phosphine to coordinate. Without the proposed half-opening of the dimer core, PPh_3 by itself appears too large to coordinate to rhenium to a measurable extent. The coordination numbers of rhenium in the intermediate would be five and six.

It appears that two structural isomers, and thus two intermediates will be formed, one that lies on the pathway for monomerization, the other on the pathway for oxygen atom transfer. The distinction lies in whether both ligands are bound to a single rhenium atom of **6**, or one ligand to reach rhenium, as shown in the transition states drawn previously. These postulates agree with the finding that four-coordinate oxo-rhenium species are sufficiently unstable to exist, even as reaction intermediates. The distinction between the two is the way in which each ternary structure facilitates subsequent reaction. For monomerization, attack on separate rhenium atoms facilitates cleavage of the one remaining μ–S bond to Re. For oxygen atom transfer, attack of the two ligands on a single rhenium results in the formation of a dioxorhenium(VII) subunit of a di-rhenium intermediate. One of the attacking groups is MeS(O)Ph, the other may be either PAr_3 (external nucleophilic assistance) or the sulfur atom of mtp (internal nucleophilic assistance).

5.3. *$AsPh_3$ in place of PPh_3*

The following reaction is spontaneous, but it proceeds with less driving force than reaction (1) does. Again, no reaction occurs without a catalyst.

$$4\text{-PicO} + AsPh_3 \rightarrow 4\text{-Pic} + Ph_3AsO,$$

$$\Delta H^\circ(\cong \Delta G^\circ) = -115\,\text{kJ(ca.)} \qquad (12)$$

We chose to explore this reaction with the reactive dimer **6** as a catalyst, in an effort to avoid the side reaction in which **6** is converted to **1**, which is much less reactive. The logic behind this is the knowledge that **6** is not converted to the monomeric species $MeReO(mtp)AsPh_3$, the analog of **1** (see reaction (7)). This is presumably so because triphenylarsine is a weaker Lewis base than triphenylphosphine. Thus the prediction was made, which proved to be so, that reaction (11) would continue to completion without loss of **6**.

Facile conversion according to reaction (11) requires the addition of Ph_3AsO. The rationale may be this: Ph_3AsO may be able to give the half-opened form of **6**, allowing coordination of MeS(O)Ph. This suggested sequence, if borne out by kinetic studies now in progress, will allow access to a transition state that provides for internal nucleophilic assistance, as depicted previously.

6. Catalysis by 8 and 9

These compounds lack a Me–Re group, being prepared directly from Re_2O_7. They are $\{ReO\}_2(mtp)_3$, **8**, and $\{ReO\}_2(edt)_3$, **9**. Studies of **8** have been completed [18].

6.1. *Phosphine coordination to catalyst **8***

Addition of PAr_3 to **8** yields a tight complex in which one of the μ(Re–S) bonds is broken, the dimeric structure being sustained by the one bridging bond remaining,

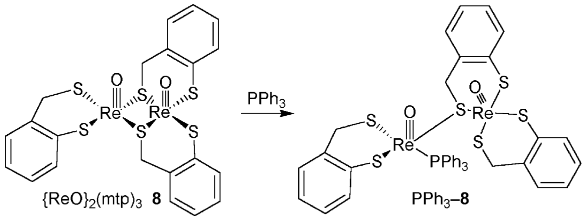

$\{ReO\}_2(mtp)_3$ **8** PPh_3–**8**

(13)

6.2. Kinetics with catalyst **8**

Even with excess phosphine, the reaction goes no further, simply because two mononuclear rhenium(V) products cannot be made thereby. Again, Re(VI) appears to be unknown in these ligand systems. Reaction (12) is not instantaneous, presumably because Re–S bond breaking accompanies Re–P bond making; the approximate rate constant is $k_{12} = 2 \times 10^4\ \mathrm{L\,mol^{-1}\,s^{-1}}$.

The rate of reaction (1) catalyzed by PPh$_3$–**8** follows this equation:

$$-\frac{\mathrm{d}[\text{Pic–O}]}{\mathrm{d}t} = \frac{k_1 k_2[\text{PPh}_3\text{–}\mathbf{8}][\text{PicO}]}{k_{-1}[\text{PicO}] + k_2[\text{PPh}_3]} \quad (14)$$

Data analysis gives $k_1 = 0.20(4)\ \mathrm{L\,mol^{-1}\,s^{-1}}$ and $k_{-1}/k_2 = 0.59$ at 25 °C in benzene. To put this catalyst on the same scale as catalysts **1** and **2**, the half-times under the conditions specified in the caption to Fig. 2 are: 32 s (**1**), 11 min (**2**), and 11 h (PPh$_3$–**8**).

6.3. Reaction mechanism for catalyst **8**

A double-labeling experiment with YPyO and XPy gave no indication that XPyO was formed, which rules out a reaction such as this because it cannot be reversible, which the rate law would require.

$$\text{Ph}_3\text{P–}\mathbf{8} + \text{PyO} \rightarrow \mathbf{16} + \text{Py} \quad (15)$$

The proposed scheme involves this sequence, where the suggested structural formulas are shown in Plate 5.

$$\mathbf{17} + \text{PyO} \underset{k_{-1}}{\overset{k_1}{\rightleftarrows}} \mathbf{18} + \text{Py} \quad (16)$$

$$\mathbf{18} + \text{PPh}_3 \xrightarrow{k2} \mathbf{17} + \text{Ph}_3\text{PO} \quad (17)$$

6.4. Phosphine reaction in a rapid step

Competition experiments that used a pair of phosphine reagents, say PY$_3$ and PZ$_3$, were used to evaluate the relative rate constant of k_2, Eq. (17). The concentrations of both of the phosphine oxides were determined as a function of time throughout the reaction. Treatment as a system of concurrent reactions affords the equation:

$$\ln\left(\frac{[\text{PY}_3]_t}{[\text{PY}_3]_0}\right) = \frac{k_Y}{k_Z}\ln\left(\frac{[\text{PZ}_3]_t}{[\text{PZ}_3]_0}\right) \quad (18)$$

The double logarithmic analysis gives the ratio of the rate constants. This method was applied to pairs of P(C$_6$H$_4$-4-X)$_3$ compounds. At the extremes, $k_{\text{OMe}}/k_{\text{CF3}} = 27$.

7. Catalysis by six-coordinate complexes

7.1. Inactive compounds

The structures of compounds **12–14** have been determined by X-ray analysis. They can be prepared by the displacement of a weaker monodentate ligand (e.g., Py) by the bidentate ligand LL and by monomerization of dimer **6** with LL:

$$\text{MeReO(mtp)Py} \xrightarrow{\text{LL}} \text{MeReO(mtp)(LL)} \xleftarrow{\text{LL}} \tfrac{1}{2}\{\text{MeReO(mtp)}\}_2 \quad (19)$$

Compounds **12–14** are inactive as catalysts for reaction (1), presumably because the tightly-bound ligands in the six-coordinate structures do not allow entry of PyO into the primary coordination shell of rhenium. The inactivity of these compounds supports the conclusion that this event is the initial step; see Schemes 1 and 2.

7.2. Catalysis by **10**

Compound **10** was specifically designed with the intention of preparing a six-coordinate complex with a bipyridine-like ligand, but one that would be less strongly bound than bpy itself. The ligand 2,2′-bipyrimidine (bpym) was selected because the two additional ring nitrogen atoms reduce its Lewis basicity.

It has been shown that **10** does indeed catalyze reaction (1). The kinetic data implicate an intermediate with a monodentate bpym, so as to allow entry of the PyO substrate [19].

7.3. Catalysis by **11**

The compound MeReO(pa)$_2$, **11**, was prepared by this reaction:

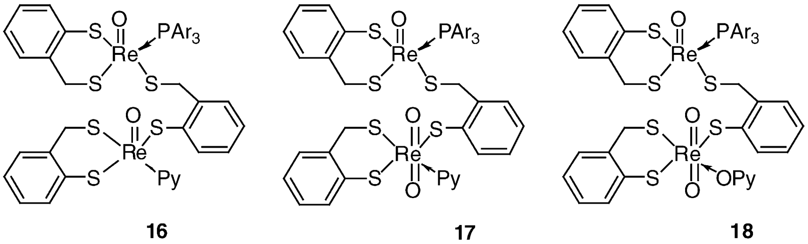

Plate 5. Structural formulas suggested for the intermediates involved in catalysis by **8**.

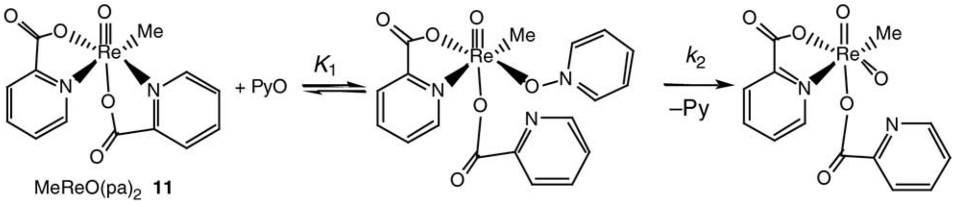

Scheme 4. Two-step reaction for catalyst **11**.

$$\mathrm{MeReO_3 + 2paH + (PPh_3/Me_2S) \rightarrow MeReO(pa)_2 + H_2O + (Ph_3PO/Me_2SO)} \quad (20)$$

Full characterization was carried out, including a single-crystal X-ray diffraction analysis which revealed the structural formula shown in Plate 3. The geometrical structure should be noted, particularly the dispositions of each O, N pair of donor atoms of pa.

Catalyst **11** was applied to this reaction:

$$\mathrm{R_2S + PyO \rightarrow R_2SO + Py} \quad (21)$$

with the result that the rate is given by

$$-\frac{\mathrm{d[PyO]}}{\mathrm{d}t} = k_\mathrm{c}[\mathrm{PyO}][\mathbf{11}] \quad (22)$$

The rate constant was independent of the identity as well as the concentration of the sulfide; $k_\mathrm{c} = 1.23 \pm 0.03\ \mathrm{L\,mol^{-1}\,s^{-1}}$ at 25 °C in anhydrous dichloromethane. For a range of ring-substituted compounds, $\mathrm{NC_5H_4X}$, pronounced substituent effects were found; from an analysis by Hammett's method, the reaction constant is $\rho = -5.2$, a remarkably large value. It seems that two reactions comprise the overall process, and that their substituent effects act in concert. This idea is embodied in Scheme 4. Consequently, $\rho_\mathrm{c} = \rho_{K1} + \rho_{k2}$; it is the two effects acting together that makes the substituent effect so large.

The kinetic data show that $\mathrm{R_2S}$ enters the mechanism in a fast step at a later stage. To explore the kinetics of that step, competition experiments were done with the pair $\mathrm{MeSC_6H_6Y/MeSPh}$. Analysis of the results by the method given in Section 4.1.3 afforded reliable values of the ratio $k_\mathrm{Y}/k_\mathrm{H}$, where these rate constants pertain to the rapid step in which an intermediate, logically the dioxorhenium(VII) species shown in Scheme 4, reacts with the thioether. The substituent effect on $k_\mathrm{Y}/k_\mathrm{H}$ is represented by $\rho = -1.9$, which supports nucleophilic attack by the thioether on an oxo oxygen.

Oxygen-18 tracer experiments were carried out with $\mathrm{MeRe^{18}O(PA)_2}$, 4-$\mathrm{Pic^{16}O}$, and $\mathrm{Me_2S}$, all at equimolar concentrations. This experiment gave $\mathrm{Me_2S^{16}O}$ only; had the thioether reacted nonselectively, there would have been 25% $\mathrm{Me_2S^{18}O}$. Scheme 5 presents a plausible explanation: catalyst **11** could not be recovered had the thioether attacked at Re = ^{18}O. Intrinsic to this mechanism are the presumptions that the pyridine nitrogen is coordinated less strongly than the carboxylate oxygen (which would form ionic species in an environment in which they are disfavored) and that the dioxorhenium(VII) intermediate must adopt a cis configuration.

8. Catalysis by 3

Compound **3**, MeReO(mtp)Py, was selected for study, anticipating that it would be more reactive than **1**, in that it has a lower barrier for ligand loss, Py being more labile that $\mathrm{PPh_3}$. Note, from Scheme 1, that ligand displacement is the first step. This expectation went unfulfilled, however, as reaction (1) started with **3**, but the reaction ceased well short of completion. We believe the problem can be traced to the intermediate $\mathrm{MeRe(O)_2(mtp)}$, **15**. As shown in Scheme 1, this species should react with $\mathrm{PPh_3}$ rapidly to complete the catalytic cycle. Analysis of the spent reaction mixture shows that neither **1** nor **3** remain. Instead, the solution contains

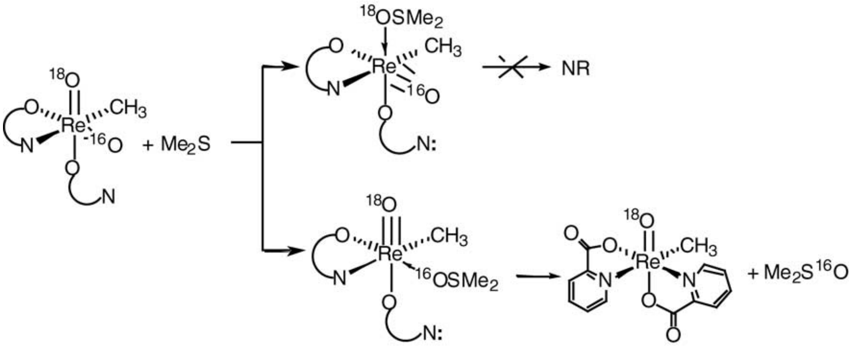

Scheme 5. Oxo-group selectivity at the thioether step.

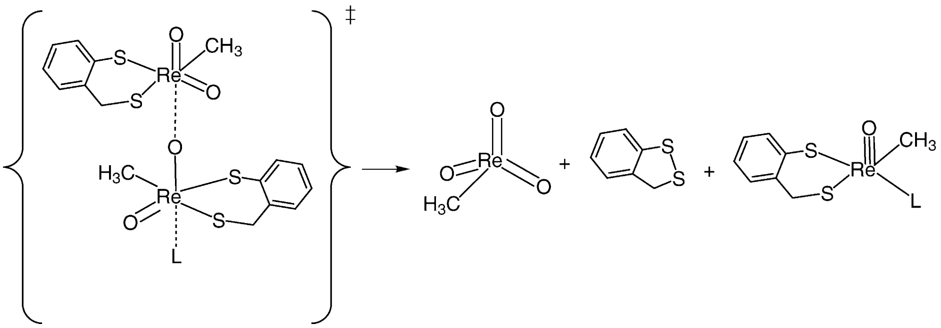

Scheme 6. Tentative mechanism for the biomolecular decomposition of dioxorhenium(VII).

$MeReO_3$ and mtp, the cyclic disulfide from the oxidation of mtp^{2-}. The net equation is

$$2MeRe(O)_2(mtp) + L \rightarrow MeReO_3 + mtp + MeReO(mtp)L$$
$$(L = PPh_3, Py) \qquad (23)$$

Circumstantial evidence suggests that **15** decomposes by second-order kinetics. As cited in Section 4.1.3, a derivative prepared at −40 °C decomposes when the solution is allowed to grow warmer. More to the point, the alkoxide-thiolate compounds $MeRe(O)_2[\kappa^2\text{-}OCH_2C(H)RS-]$, R = H or Me[16] can be studied in solution but pure compounds could not be isolated. If, indeed, **15** decomposes by second-order kinetics, then the more labile Py catalyst **3** will produce the intermediate at a higher steady-state concentration. Thus a competition will be established between the reactions of **15** with PPh_3 and with itself, which quickly brings catalysis to a halt.

As to the mechanism whereby **15** self-destructs, Eq. (23), we suggest on the grounds of plausibility the transition state shown in Scheme 6, but can advance no experimental data to support it.

9. Unifying mechanistic aspects

Each of the catalysts for reactions (1), (8), and (20) gives rise to a different rate equation. This article has summarized the applicable forms and set forth for each the sequence of reactions that can be deduced from the kinetics. Indeed, the differences among the oxo- and thio-rhenium(V) catalysts have been the principal issues emphasized in the preceding sections.

Examination of the transition states that have been drawn clearly shows that all of the reactions have much more in common than the principal theme that each catalyst gives rise to a different rate equation would imply. In every case, the substantial barrier is the breaking of the Py–O or R_2S–O bonds, an event that is compensated by formation of the dioxorhenium(VII) intermediate. Also, for each of the catalysts, the data show that an additional nucleophilic reagent is needed to complete the overall reaction. One way to represent the structure of a transition state that brings out the common factor can be shown as follows:

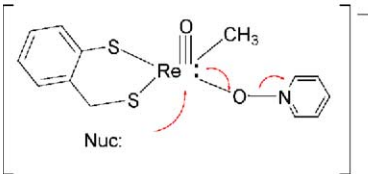

All of the reactions described herein attain this transition state, even though each arrives there differently. As remarked earlier, substituent effects were used to demonstrate that Py–O bond breaking is not far advanced in the transition state; that is, it is an early transition state.

Having explored the differences that stimulated the extensive experimental work, it is gratifying to see that the data do point to a unifying view of the mechanism at the critical step of the transformation.

Acknowledgments

Many aspects of the research reviewed here was supported by the US Department of Energy, Office of Basic Energy Sciences, Division of Chemical Sciences under contract W-7405-Eng-82 with Iowa State University of Science and Technology. Other portions of the work were supported by the National Science Foundation. I am grateful to Professors R.J. Angelici and W.P. Giering for helpful discussions.

References

[1] (a) D. Katakis, H. Taube, J. Chem. Phys. 36 (1962) 416;
(b) H. Taube, Transact. Faraday Soc. 53 (1957) 656;
(c) O.L. Forchheimer, H. Taube, J. Am. Chem. Soc. 76 (1954) 2099;
(d) L.R.B. Yeatts Jr., H. Taube, J. Am. Chem. Soc. 71 (1949) 4100;
(e) H. Taube, J. Am. Chem. Soc. 64 (1942) 2468.
[2] (a) W. Kruse, H. Taube, J. Am. Chem. Soc. 83 (1961) 1280;
(b) M. Anbar, H. Taube, J. Am. Chem. Soc. 80 (1958) 1073;
(c) M. Anbar, H. Taube, J. Am. Chem. Soc. 76 (1954) 6243;
(d) O.L. Forchheimer, H. Taube, J. Am. Chem. Soc. 74 (1952) 3705;
(e) J. Halperin, H. Taube, J. Am. Chem. Soc. 72 (1950) 3319;
(f) H. Taube, Rec. Chem. Prog. 17 (1956) 25.

[3] (a) R.M. Milburn, H. Taube, J. Phys. Chem. 64 (1960) 1776;
(b) P. Saffir, H. Taube, J. Am. Chem. Soc. 82 (1960) 13;
(c) R.M. Milburn, H. Taube, J. Am. Chem. Soc. 81 (1959) 3515;
(d) H. Taube, J. Am. Chem. Soc. 70 (1948) 3928;
(e) I.L. Hochhauser, H. Taube, J. Am. Chem. Soc. 69 (1947) 1582;
(f) H. Taube, J. Am. Chem. Soc. 69 (1947) 1418.

[4] (a) G. Gordon, H. Taube, J. Inorg. Nucl. Chem. 16 (1961) 272;
(b) A.C. Rutenberg, H. Taube, J. Chem. Phys. 20 (1952) 825;
(c) R.A. Plane, H. Taube, J. Phys. Chem. 56 (1952) 33;
(d) J.P. Hunt, H. Taube, J. Chem. Phys. 19 (1951) 602;
(e) J.P. Hunt, H. Taube, J. Chem. Phys. 18 (1950) 757;
(f) H.L. Friedman, H. Taube, J.P. Hunt, J. Chem. Phys. 18 (1950) 759.

[5] J.H. Espenson, H. Taube, Inorg. Chem. 4 (1965) 704.

[6] W.P. Jencks, Chem. Soc. Rev. 10 (1981) 345.

[7] (a) E. Ochiai, J. Org. Chem. 18 (1953) 354;
(b) T. Rosenau, A. Potthast, G. Ebner, P. Kosma, Synletter 6 (1999) 623.

[8] (a) E. Ochiai, Aromatic Amine Oxides, Elsevier Publishing Co, Amsterdam, 1967;
(b) A.R. Katritzky, J.M. Lagowski, In Organic Chemistry, A Series of Monographs, Academic Press, New York, 1971;
(c) B.M. Trost, L. Fleming, Comprehensive Org. Synth. 8 (1991) 390.

[9] M.D.M.C. Ribeiro da Silva, M. Agostinha, R. Matos, M.C. Vaz, L.M.N.B.F. Santos, G. Pilcher, W.E. Acree Jr., J.R. Powell, J. Chem. Thermodyn. 30 (1998) 869.

[10] D.C. Palmer, Version 4.1 ed., CrystalMaker Software, Oxford, Bicester, UK, 2001.

[11] Y. Wang, J.H. Espenson, Inorg. Chem. 41 (2002) 2266.

[12] K. Osz, J.H. Espenson, Inorg. Chem. 42 (2003) 8122.

[13] J. Jacob, G. Lente, I.A. Guzei, J.H. Espenson, Inorg. Chem. 38 (1999) 3762.

[14] (a) J.H. Espenson, S.M. Nabavizadeh, Eur. J. Inorg. Chem. (2003) 1911;
(b) X. Shan, J.H. Espenson, Organometallics 22 (2003) 1250;
(c) X. Shan, A. Ellern, J.H. Espenson, Inorg. Chem. 41 (2002) 7136;
(d) J.H. Espenson, X. Shan, D.W. Lahti, T.M. Rockey, B. Saha, A. Ellern, Inorg. Chem. 40 (2001) 6717;
(e) G. Lente, J. Jacob, I.A. Guzei, J.H. Espenson, Inorg. React. Mech. 2 (2000) 169;
(f) G. Lente, I.A. Guzei, J.H. Espenson, Inorg. Chem. 39 (2000) 1311.

[15] D.W. Lahti, J.H. Espenson, J. Am. Chem. Soc. 123 (2001) 6014.

[16] J. Dixon, J.H. Espenson, Inorg. Chem. 41 (2002) 4727.

[17] N. Koshino, J.H. Espenson, Inorg. Chem. 42 (2003) 5735.

[18] R. Huang, J.H. Espenson, Inorg. Chem. 40 (2001) 994.

[19] Y. Cai, J.H. Espenson, unpublished information.